Highly Sensitive Quinoline-Based Two-Photon Fluorescent Probe for Monitoring Intracellular Free Zinc Ions

ARTICLE *in* ANALYTICAL CHEMISTRY · MAY 2014

Impact Factor: 5.64 · DOI: 10.1021/ac501947v · Source: PubMed

6 AUTHORS, INCLUDING:

Zhiqiang Mao
Wuhan University
3 PUBLICATIONS **10** CITATIONS
SEE PROFILE

Liang Hu
Wuhan Institute of Physics and Mathematics
8 PUBLICATIONS **20** CITATIONS
SEE PROFILE

Cheng Zhong
Wuhan University
89 PUBLICATIONS **2,031** CITATIONS
SEE PROFILE

analytical chemistry

Article

pubs.acs.org/ac

Highly Sensitive Quinoline-Based Two-Photon Fluorescent Probe for Monitoring Intracellular Free Zinc Ions

Zhiqiang Mao,[†] Liang Hu,[‡] Xiaohu Dong,[§] Cheng Zhong,[∥] Bi-Feng Liu,[‡] and Zhihong Liu*,[†]

[†]Key Laboratory of Analytical Chemistry for Biology and Medicine (Ministry of Education), College of Chemistry and Molecular Sciences, Wuhan University, Wuhan, Hubei 430072, China

[‡]Britton Chance Center for Biomedical Photonics at Wuhan National Laboratory for Optoelectronics-Hubei Bioinformatics & Molecular Imaging Key Laboratory, Systems Biology Theme, Department of Biomedical Engineering, College of Life Science and Technology, Huazhong University of Science and Technology, Wuhan, Hubei 430074, China

[§]Xi'an Modern Chemistry Research Institute, Xi'an, Shaanxi 710065, China

[∥]Hubei Key Laboratory on Organic and Polymeric Optoelectronic Materials, College of Chemistry and Molecular Sciences, Wuhan University, Wuhan, Hubei 430072, China

Supporting Information

ABSTRACT: Zn^{2+} plays vital roles in regulating physiological and pathological processes. A number of diseases are associated with the disruption of intracellular free Zn^{2+} homeostasis, and the relationship is still uncovered. Thus, it is important to monitor intracellular free Zn^{2+} ions in real time, which is still challenging due to the low content of intracellular free Zn^{2+}. In this work, we report on the design and synthesis of a new two-photon (2P) fluorescent probe, QZn, based on quinoline derivative for intracellular free Zn^{2+}. Theoretical calculations were carried out to rationalize the design. The probe displayed a moderate 2P action cross section value of 51 GM at 820 nm and up to 10-fold fluorescence enhancement upon Zn^{2+} binding. The detection limit of Zn^{2+} was 15.1 pM, which presented a pronounced sensitivity toward Zn^{2+} and indicated that QZn would be competent for detecting the low-content intracellular Zn^{2+}. By using two-photon microscopy, QZn was capable of monitoring the fluctuation of intracellular free zinc ions in real time.

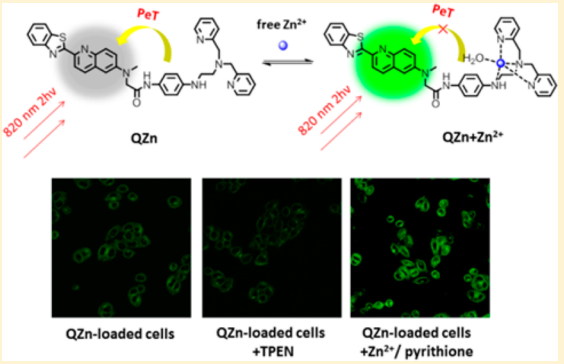

Zinc is one of the most abundant nutritionally essential elements in the human body.[1] The indispensable roles of Zn^{2+} in a variety of cellular systems including the redox state, enzymatic function, and cellular signaling have been well recognized.[2−4] Deficiency or an extreme excess of intracellular free Zn^{2+} has been considered to be associated with a number of diseases, such as Alzheimer's disease, Parkinson's disease, diabetes, and immune dysfunction.[5,6] Recently, intracellular free Zn^{2+} regarded as a biomarker for prostate cancer has also been reported.[7] To acquire better understanding of the roles of Zn^{2+} in biological systems, it is important to monitor the distribution and concentration of free Zn^{2+} in cells in real time. While the total concentration of cellular zinc is estimated to be as high as 0.2 mM, the cytosol contains a labile pool of free Zn^{2+} at only picomolar to nanomolar levels.[8] Therefore, highly sensitive and reliable approaches to the detection of intracellular Zn^{2+} are desired.

The fluorescent probe is regarded as an excellent tool to monitor the amount and activity of intracellular species due to its high selectivity, high sensitivity, and low damage to biological samples. So far, a number of fluorescent probes has been developed for Zn^{2+}, which consist of diverse fluorophores and Zn^{2+} receptors, and has been applied in intra- or extracellular zinc probing.[9−15] Despite the great contributions of these elegant works, however, most of the reported probes work under one-photon excitation at wavelengths less than 550 nm. These down-conversion fluorophores with relatively short excitation wavelengths are likely to be subject to several problems, such as the cellular autofluorescence, the photobleaching of probes, and limited penetration depth of the excitation light. These issues may impair the biological applications of these fluorescent probes, for example, the long-term observation of the fluctuation of intracellular free Zn^{2+}.

An effective alternative to circumvent the drawbacks of one-photon excitation probing is the utilization of two-photon microscopy (2PM) with two-photon excitable probes. 2PM takes two photons of lower energy for the excitation. Compared to one-photon microscopy, 2PM has been proven for its advantages of less phototoxicity, longer observation time, better temporal and spatial resolution, and larger penetration depth

Received: March 24, 2014
Accepted: May 30, 2014
Published: May 30, 2014

   dx.doi.org/10.1021/ac501947v | *Anal. Chem.* 2014, 86, 6548−6554

Scheme 1. Synthesis of QZn[a]

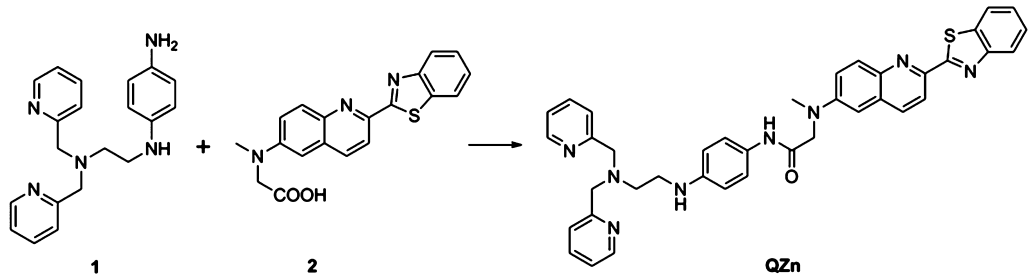

[a]Reagents and conditions: DCC, HOBt, CH_2Cl_2.

(>500 μm).[16,17] Hence, it is a powerful technique that can visualize biological substances (or their activities) intact in live cells for a long period and has gained rapid development in the past decade. Nevertheless, a limitative factor of 2-photon microscopy is the lack of efficient two-photon scaffolds to develop two-photon fluorescent probes. Over the past several years, considerable efforts have been carried out to provide new fluorophores with large two-photon cross sections (δ), but due to the difficulty in finding the right balance between the optical properties and the biological constraints, currently, the challenge still remains quite topical. To date, only a few two-photon fluorescent probes based on benzoxazole,[18] stilbene,[19] and naphthalene derivatives[20−22] for Zn^{2+} have been developed. Due to the low content of intracellular free Zn^{2+}, novel 2P probes with high sensitivity are still in great need. Recently, our group proposed a new two-photon fluorophore using a quinoline scaffold,[23] which possesses favorable photophysical properties and is easy to be modified at the 2,6 positions. Herein in this work, on the basis of the derivation of the quinoline motif as well as theoretical calculation, we designed and prepared a new two-photon Zn^{2+} probe, QZn, composed of a quinoline derivative as the 2P fluorophore and *N*,*N*-di(2-picolyl)ethylenediamine (DPEN) as the Zn^{2+} acceptor, with which the real-time monitoring of intracellular free Zn^{2+} with high sensitivity by 2PM was achieved.

EXPERIMENTAL SECTION

Materials and Apparatus. All solvents and reagents were used as received without further purification unless for special needs. All aqueous solutions were prepared in ultrapure water with a resistivity of 18.25 MΩ·cm (purified by the Milli-Q system supplied by Millipore). Two-photon excited fluorescence data were measured by exciting with a mode-locked Ti:sapphire femtosecond pulsed laser (Chameleon Ultra I, Coherent Inc.) with a pulse width of 140 fs and repetition rate of 80 MHz. The two-photon excited fluorescence intensity was recorded on a DCS200PC Photon Counting (Beijing Zolix Instruments Co., Ltd.) with single-photon sensitivity through an Omni-λ5008 monochromator (Beijing Zolix Instruments Co., Ltd.). One-photon excited fluorescence was measured on a RF-5301 fluorescence spectrophotometer (Shimadzu Scientific Instruments Inc.). Absorption measurements were conducted on a UV2550 UV−vis spectrophotometer (Shimadzu Scientific Instruments Inc.). Two-photon microscopy of HeLa cells was performed on a Zeiss Axio Examiner LSM 780 multiphoton laser scanning confocal microscope (Carl Zeiss, Germany).

Synthesis of QZn is described as below (Scheme 1). Compounds **1** and **2** were prepared according to the literature method.[20,23]

Synthesis of QZn. A mixture of **2** (0.10 g, 0.29 mmol), 1-hydroxybenzotriazole (0.043 g, 0.32 mmol), 1,3-dicyclohexyl carbodiimide (0.057 g, 0.28 mmol) in dichloromethane was stirred for 1 h. To this mixture, **1** (0.11 g, 0.33 mmol) was added and stirred for 18 h under N_2. The product was extracted with dichloromethane and dried over Na_2SO_4, and the solvent was removed in vacuo. The product was purified by column chromatography using chloroform/methanol (50:3) as the eluent. It was further purified by recrystallization from $CHCl_3$/petroleum ether. Yield 0.096 g (50%) of yellow powder; mp 156 °C. ^{1}H NMR (400 MHz, $CDCl_3$) δ 8.54 (d, J = 4.3 Hz, 2H), 8.39 (d, J = 8.6 Hz, 1H), 8.17−8.07 (m, 3H), 8.05 (s, 1H), 7.98 (d, J = 7.9 Hz, 1H), 7.63−7.59 (m, 2H), 7.51 (t, J = 7.2 Hz, 1H), 7.46−7.35 (m, 4H), 7.25 (s, 1H), 7.18−7.09 (m, 2H), 7.00 (d, J = 2.7 Hz, 1H), 6.53 (d, J = 8.8 Hz, 2H), 4.79 (s, 1H), 4.12 (s, 2H), 3.86 (s, 4H), 3.24 (s, 3H), 3.12 (t, J = 5.7 Hz, 2H), 2.85 (t, J = 5.8 Hz, 2H). ^{13}C NMR (100 MHz, DMSO-d_6) δ 170.20, 167.47, 159.15, 154.36, 149.13, 148.03, 146.31, 142.60, 136.50, 136.22, 135.08, 130.31, 125.61, 121.99, 119.58, 118.90, 112.95, 106.63, 60.27, 59.20, 52.74, 41.65, 33.97. HRMS (MALDI) Cacld. for $C_{39}H_{37}N_8OS$ $[M + H]^+$: 665.2799. Found 665.2805.

Theoretical Calculation. Geometries of QZn and QZn-Zn^{2+} were optimized at B3LYP/6-31G (d) level with LanI2dz pseudopotential basis set for Zn. The integral equation formalism polarizable continuum model (IEFPCM) was used to account for the effect of solvation by water. Then, the molecule orbitals were extracted from an electronic structure calculated at same level of theory. All the calculations were performed using the Gaussian 09 program.[24]

Measurement of Two-Photon Cross Section. The two-photon cross section (δ) was determined by using the femtosecond fluorescence measurement technique as described.[25−27] QZn (1.0×10^{-6} M) was dissolved in 30 mM MOPS buffer (100 mM KCl, pH = 7.2, 10 mM EGTA, 1% DMSO), and the two-photon induced fluorescence intensity was measured in the range from 760 to 860 nm by using rhodamine B (1×10^{-6} M) in methanol as the reference. The two-photon fluorescence property of rhodamine B has been well characterized in the literature.[28] The intensities of the two-photon induced fluorescence of the reference and sample were detected at the same excitation wavelength. The 2P absorption cross section was calculated by using $\delta_s = \delta_r[S_s\Phi_r(n_s)^2c_r]/[S_r\Phi_s(n_r)^2c_s]$: where the subscripts s and r stand for the sample and reference molecules, respectively. The intensity of the two-photon excited fluorescence is denoted as S. Φ is the fluorescence quantum yield,[29] and n is the refractive index of the solvent. The number density of the molecules in solution is

dx.doi.org/10.1021/ac501947v | Anal. Chem. 2014, 86, 6548−6554

denoted as *c*. δ_r is the 2P cross section of the reference molecule.

Two-Photon Fluorescence Imaging in HeLa Cells. HeLa cells were obtained from College of Life Science and Technology, Huazhong University of Science and Technology. Before the imaging experiments, the viability of cells was examined using the CCK-8 kit (Cell Counting Kit-8, Dojindo, Japan) according to the manufacture's protocol. In a typical fluorescence imaging procedure, cells were cultured with Dulbecco's modified Eagle's medium (DMEM) supplemented with 10% (v/v) newborn calf serum (Gibco), 100 U·mL^{-1} penicillin, and 100 μg·mL^{-1} streptomycin in a humidified atmosphere with 5/95 (v/v) of CO_2/air at 37 °C. One day before imaging, cells were detached with a treatment of 0.2% (w/v) trypsin-EDTA solution (Gibco) and suspended in culture media. The cell suspension was then transferred to confocal dishes to grow with adherence. For labeling, the growth medium was replaced with 0.5 μM QZn in culture media and incubated at 37 °C under 5% CO_2 for 30 min. Then, the cells were washed three times with phosphate buffered saline (PBS; Gibco). After the cells were incubated with 25 μM *N*,*N*,*N*′,*N*′-tetrakis(2-pyridyl)ethylenediamine (TPEN) and 50 μM $ZnCl_2$/pyrithione (2-mercaptopyridine *N*-oxide) (1:1), respectively, for another 30 min at 37 °C, the HeLa cells were washed with PBS three times again. The two-photon fluorescence microscopy images were obtained with a multiphoton laser scanning confocal microscope (Zeiss Axio Examiner, LSM 780) by exciting the probe with a Mai Tai HP (690−850 nm) femtosecond pulse laser set at 820 nm (Newport Corporation, US).

RESULTS AND DISCUSSION

Design of QZn. The two-photon photophysical property and biocompatibility are the two essential concerns when designing a 2P probe. We selected quinoline as the fluorophore scaffold in consideration of its rigid structure. To further enlarge the conjugate plane and the polarity of the molecule, an electron acceptor benzothiazole and an electron donor amino group were introduced to the 2,6 position of quinoline, respectively, so as to form a typical D-π-A structure.[30−34] Such a rigid conjugated D-π-A structure with large polarity is in favor of 2P optical properties.[35−38] *N*,*N*-Di(2-picolyl)-ethylenediamine (DPEN) was chosen as Zn^{2+} receptor for its strong binding affinity toward zinc ions.[39−41] Meanwhile, the hydrophilic pyridine group is anticipated to improve the water solubility of QZn to some extent. We adopted a photoinduced electron transfer (PeT) mechanism so that QZn would show a great fluorescence enhancement in response to zinc ions through the blocking of the PeT process (Scheme 2). The rationality of the PeT design was confirmed by theoretical calculations using Gaussian 09 (DFT in B3LYP/6-31G (d) level). The calculation results are shown in Figure 1. The optimized structure of the compounds revealed that the QZn-Zn^{2+} complex is with a structure of trigonal bipyramid, in which Zn^{2+} ion is coordinated by four nitrogen atoms and one water molecule. For QZn, the HOMO (highest occupied molecular orbital) mainly distributes in *p*-benzenediamine moiety and both the LUMO (lowest unoccupied molecular orbital) and HOMO-1 mainly localize in the fluorophore moiety (Figure 1a). Upon the excitation of free QZn, electrons transfer from the receptor to the fluorophore, impeding the radiative relaxation and thus resulting in fluorescence quenching which can be confirmed by the TD-DFT calculated small oscillator

Scheme 2. Structure of QZn and Illustration of the Zn^{2+} Sensing Process

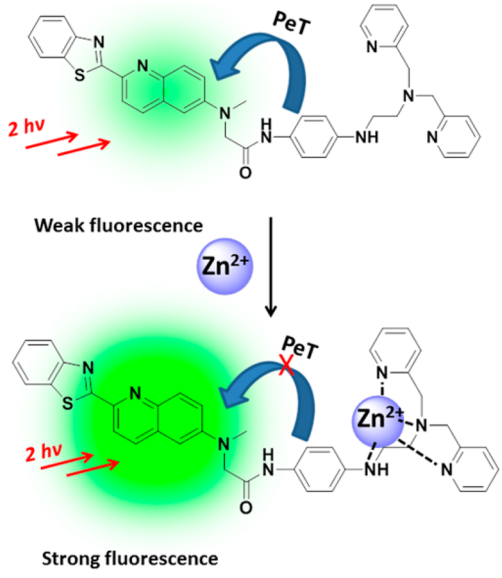

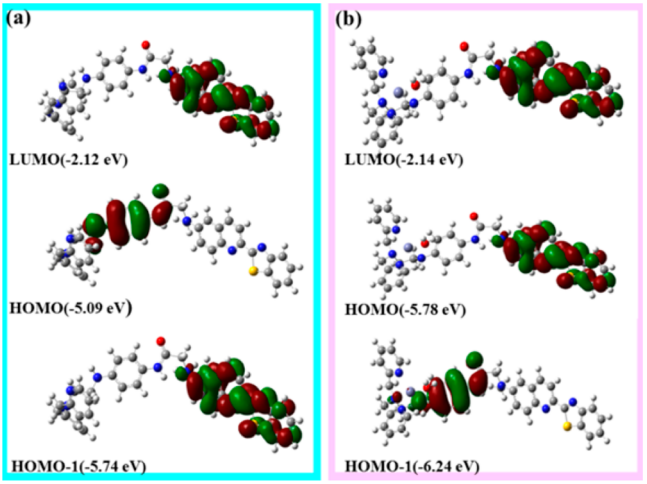

Figure 1. Geometries and frontier orbitals of (a) QZn and (b) QZn-Zn^{2+}.

strength of the first singlet excited state of QZn (0.0034) (Table S3 in the Supporting Information). After coordinating with Zn^{2+}, the level of HOMO that locates on *p*-benzenediamine moiety decreases from −5.09 to −6.24 eV; as a result, HOMO in QZn becomes HOMO-1 in QZn-Zn^{2+} and both HOMO and LUMO mainly lie on the fluorophore moiety (Figure 1b); therefore, no electron transfers from the *p*-benzenediamine moiety to the fluorophore moiety under excitation, and the fluorescence is intensified upon binding with Zn^{2+}. These processes are in agreement with a-PeT mechanism mediated fluorescence change (fluorophore as the electron acceptor in PeT).[42,43]

Fluorometric Detection of Zn^{2+} with QZn. The photophysical data of QZn were obtained in 30 mM 3-(*N*-morpholino)propanesulfonic acid (MOPS) buffer (100 mM KCl, pH = 7.2, 10 mM EGTA, containing 1% DMSO). The water solubility of QZn was first determined in the aqueous solution, which was about 4.0 μM in MOPS buffer, a value adequate for solution-phase detection and cell staining (Figure S1 in the Supporting Information). Free QZn showed

dx.doi.org/10.1021/ac501947v | Anal. Chem. 2014, 86, 6548−6554

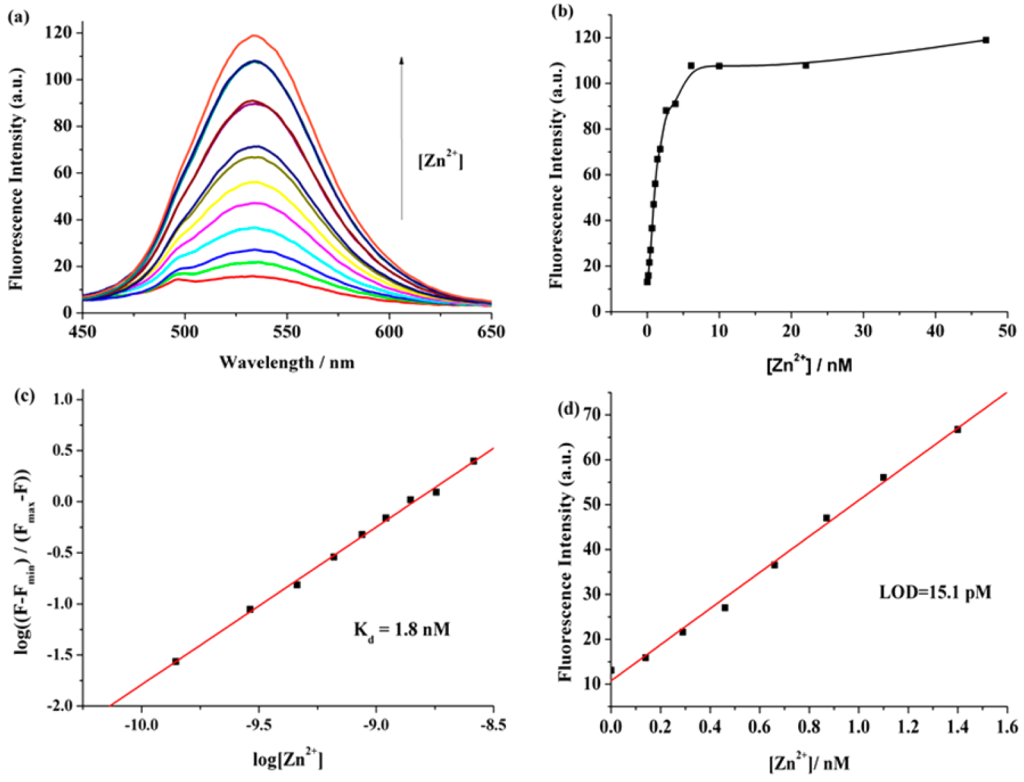

Figure 2. (a) One-photon fluorescence spectra of 1 μM QZn in the presence of varying amounts of free Zn^{2+} (0–47 nM). (b) One-photon fluorescence titration curve for the complexation of QZn with free Zn^{2+} (0–47 nM). (c) Hill plot for the complexation of QZn with free Zn^{2+}. (d) Plot of fluorescence intensity as a function of free Zn^{2+} (0.14–1.40 nM). The excitation wavelength was 419 nm, and the fluorescence intensity was measured at 537 nm. These data were measured in 30 mM MOPS buffer (100 mM KCl, pH = 7.2, 10 mM EGTA, containing 1% DMSO).

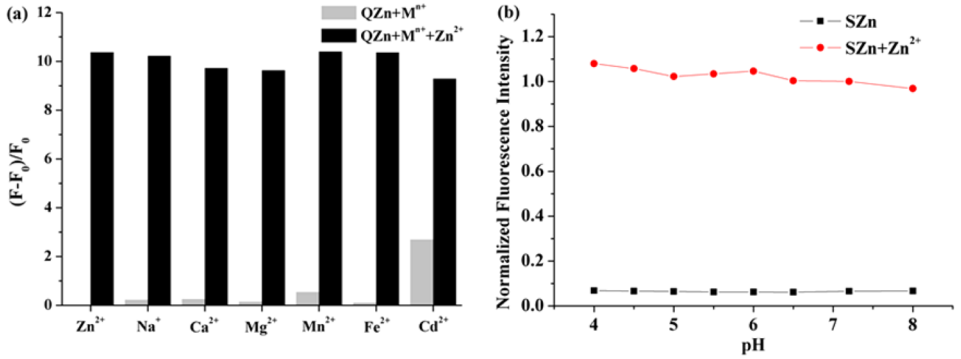

Figure 3. (a) The relative fluorescence intensity of 1.0 μM QZn in the presence of 1.0 mM Na^+, Ca^{2+}, and Mg^{2+}; 1.0 μM Mn^{2+}, Fe^{2+}, and Cd^{2+} (gray bars) followed by addition of 1 μM Zn^{2+} (black bars) in 30 mM MOPS buffer (100 mM KCl, pH = 7.2, containing 1% DMSO). (b) Effect of pH on the one-photon fluorescence intensity of 1 μM QZn in the absence and presence of 47 nM free Zn^{2+} in 30 mM MOPS buffer (100 mM KCl, pH = 7.2, 10 mM EGTA, containing 1% DMSO). The excitation wavelength was 419 nm, and the fluorescence intensity was measured at 537 nm.

absorption and emission maxima at 417 nm (ε = 2.2 × 10^4 $M^{-1}\cdot cm^{-1}$) and 533 nm, respectively. As expected, it was weakly fluorescent with a low quantum yield (Φ = 0.012). Upon addition of Zn^{2+}, the fluorescence intensity increased dramatically and showed a slight red shift in both its absorption (419 nm, ε = 2.8 × 10^4 $M^{-1}\cdot cm^{-1}$) and emission maxima (537 nm, Φ = 0.18) (Figure S2 and Table S2 in the Supporting Information). These experimental results were consistent with theoretical calculations and rationalized the concept of the PeT process.[44−48] Because of the large polarity of the molecule resulting from the D-π-A structure, the emission spectra showed obvious bathochromic shifts with the increase of solvent polarity (Figure S3 in the Supporting Information).

The fluorescence titration of QZn by free Zn^{2+} is illustrated in Figure 2a. After reaching the plateau, the fluorescence enhancement factor ($(F_{max} - F_0)/F_0$) of QZn with excess Zn^{2+} was ca. 10-fold (Figure 2b). The dissociation constant (K_d) between QZn and Zn^{2+} calculated from the fluorescence titration curve was 1.8 nM (Figure 2c), which was much smaller than that of previous reported two-photon Zn^{2+} probes[18,19] and indicated QZn had a tight binding affinity toward zinc ions. The fluorescence of the probe exhibited a linear response to Zn^{2+} concentration in the range of 0.14–1.40 nM (Figure 2d), from which the limit of detection (LOD) for Zn^{2+} was experimentally determined to be 15.1 pM. The result suggested

dx.doi.org/10.1021/ac501947v | Anal. Chem. 2014, 86, 6548−6554

that QZn was highly sensitive to Zn^{2+} and could be suitable for monitoring the low-level intracellular free Zn^{2+}.

Specificity and pH Dependence of QZn. The selectivity of QZn toward Zn^{2+} was investigated through measuring the fluorescence intensity of QZn in the presence of Zn^{2+} and other biologically relevant metal ions. As shown in Figure 3a, the Zn^{2+}-induced fluorescence enhancement ($(F - F_0)/F_0$) was up to 10-fold, while QZn showed no obvious fluorescence intensity change toward other metal ions (with a concentration as high as 1 mM) except for Cd^{2+}, which caused a fluorescence enhancement ca. 30% to that of Zn^{2+}. When the target Zn^{2+} was coexistent with these interfering ions, the signal alteration was less than 10% for all the ions. These results showed acceptable selectivity of QZn for Zn^{2+} over other metal ions. To guarantee the intracellular usage of the probe, we also evaluated the pH dependence of QZn and QZn-Zn^{2+} complex. In the pH range of 4.0−8.0, no significant change in the emission intensity at 537 nm was observed for the free probe or the complex (Figure 3b), indicating that the substances were pH insensitive and that QZn could be applicable in the biologically relevant pH range.

Two-Photon Fluorescence Properties of QZn. The two-photon action cross section ($\Phi\delta$) of a 2P probe is of prime importance for its 2PM application, which decides the signal-to-noise ratio and imaging sensitivity. The 2P action cross section spectra of QZn and QZn-Zn^{2+} complex were determined in 30 mM MOPS buffer (100 mM KCl, pH = 7.2, 10 mM EGTA) with rhodamine B as the reference. Owing to the efficient PeT process as discussed above, the probe QZn itself showed very weak 2P fluorescence and the action cross section was not detectable, while the complex QZn-Zn^{2+} exhibited favorable $\Phi\delta$ values with a maximum of 51 GM at 820 nm (Figure S4 in the Supporting Information). The fluorescence intensity showed a quadratic dependence on excitation power at 820 nm, which proved that the photoluminescence was from a two-photon process (Figure S5 in the Supporting Information). The photostability of QZn was tested in QZn-labeled HeLa cells, which revealed that the 2P fluorescence intensity of QZn-Zn^{2+} did not change even after continuous irradiation by an 820 nm femtosecond laser for 40 min (Figure S6 in the Supporting Information). These results showed that QZn was able to afford bright 2P fluorescence during a long period of observation with a negligible photobleaching problem.

Imaging of Free Zn^{2+} in Live Cells. Before we moved on to utilize QZn as a 2P probe for tracking free Zn^{2+} in living cells, we assessed the cytotoxicity of QZn by using CCK-8 kit. HeLa cells were treated with various concentrations (5−30 μM) of QZn for 4 h. As shown in Figure 4, high cell viability was maintained as compared to the control, which demonstrated a low cytotoxicity of the probe. For the cell imaging experiments, HeLa cells were first incubated with 0.5 μM QZn for 30 min. The green fluorescence uniformly distributing in the cytoplasm region indicated the efficient loading of the probe and possible tracking of intracellular free Zn^{2+} (Figure 5a). The uniform distribution of QZn in the cytoplasm region can be confirmed by 3D images of spatial localization of QZn in HeLa cells (Figure S7 in the Supporting Information). Meanwhile, no fluorescence was observed in the extracellular environment, suggesting minimized leaking out of the probe. To confirm that the observed fluorescence was induced by intracellular free zinc ions, a well-known cell membrane-permeable Zn^{2+} chelator, *N*,*N*,*N*′,*N*′-tetrakis(2-pyridyl)-ethylenediamine (TPEN),[49−52] was added to QZn-loaded HeLa cells. In this situation, the 2P excited fluorescence

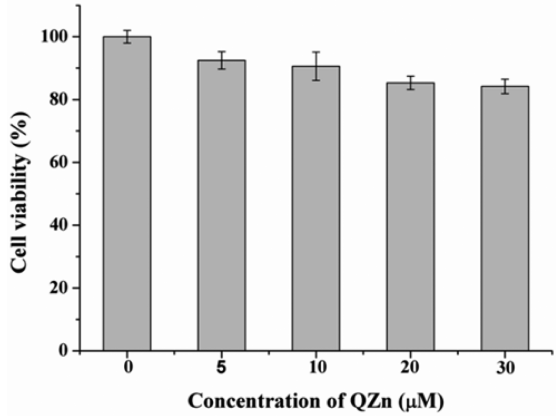

Figure 4. Viability of HeLa cells in the presence of QZn as measured by the CCK-8 kit. The HeLa cells were incubated with different concentrations of QZn for 4 h.

intensity of the cells decreased substantially after the treatment with 25 μM TPEN (Figure 5b). It is explained that TPEN competed with QZn to capture intracellular free Zn^{2+}, leading to the fluorescence intensity decrease. To further evaluate whether this probe can monitor intracellular free Zn^{2+} fluctuation, a solution of $ZnCl_2$ and pyrithione (2-mercaptopyridine *N*-oxide) complex (1:1) was added to the QZn-loaded HeLa cells. Consequently, a remarkable fluorescence enhancement was observed (Figure 5c). It could be interpreted that $ZnCl_2$/pyrithione (1:1) complex entered into cytoplasm and released free Zn^{2+} ions,[53] so that QZn responded to the elevated level of free Zn^{2+} in cells and exhibited brighter fluorescence. Moreover, intracellular free Zn^{2+} can also be qualitatively measured according to the average two-photon excited fluorescence intensities of QZn-loaded cells (Figure 5d).

The above results proved that QZn can selectively and sensitively monitor the fluctuation of intracellular free Zn^{2+} in living cells under incubation conditions. Encouraged by the results, we sought to utilize QZn to monitor the intracellular zinc ions level in real time by 2PM. As shown in Figure 6, the 2PEF intensity did not change until the cells were treated with 2,2-dithiodipyridine (DTDP; 150 μM), a reagent that promotes the release of free Zn^{2+} from Zn^{2+} binding proteins.[54] After the addition of DTDP, the 2PEF intensity increased gradually and reached the plateau in ca. 3 min (Figure 6a,b). Hereafter, upon addition of 50 μM TPEN, the 2PEF intensity decreased to another plateau rapidly (Figure 6c). The real-time change of the intracellular free Zn^{2+} level was reflected distinguishingly from the plot of 2PEF intensity versus time (Figure 6d). The results revealed that QZn could dynamically monitor the intracellular zinc ions level in real time due to the reversible Zn^{2+} binding and neglectable photobleaching. All these results suggested that QZn might be applied as a powerful tool to study Zn^{2+} roles in physiology and pathology by two-photon microscopy.

CONCLUSIONS

In summary, a new 2P probe (QZn) for Zn^{2+} with a quinoline derivative as 2P fluorophore was designed and prepared. The design was rationalized by theoretical calculations. The probe showed high sensitivity for Zn^{2+} in aqueous buffer with a LOD of 15.1 pM. Moreover, QZn also featured a highly selective response to Zn^{2+} over other biological metal ions, good water

dx.doi.org/10.1021/ac501947v | *Anal. Chem.* 2014, 86, 6548−6554

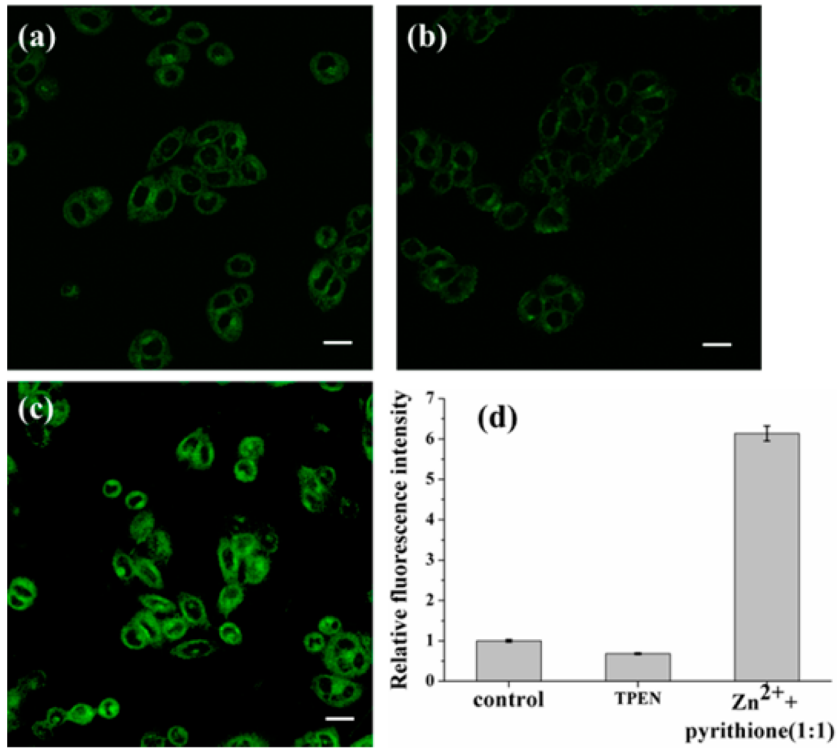

Figure 5. 2P images of HeLa cells labeled with QZn. (a) 2P images of HeLa cells incubated with QZn (0.5 μM) for 30 min. (b) 2P images of HeLa cells incubated with QZn (0.5 μM) for 30 min and then with 25 μM TPEN for another 30 min. (c) 2P images of HeLa cells incubated with QZn (0.5 μM) for 30 min and then with 50 μM $ZnCl_2$/pyrithione (1:1) solution for another 30 min. (d) Average two-photon excited fluorescence intensities in (a–c). Scale bar: 20 μm. The 2PEF data were collected at 500–570 nm upon excitation at 820 nm with a femtosecond pulse.

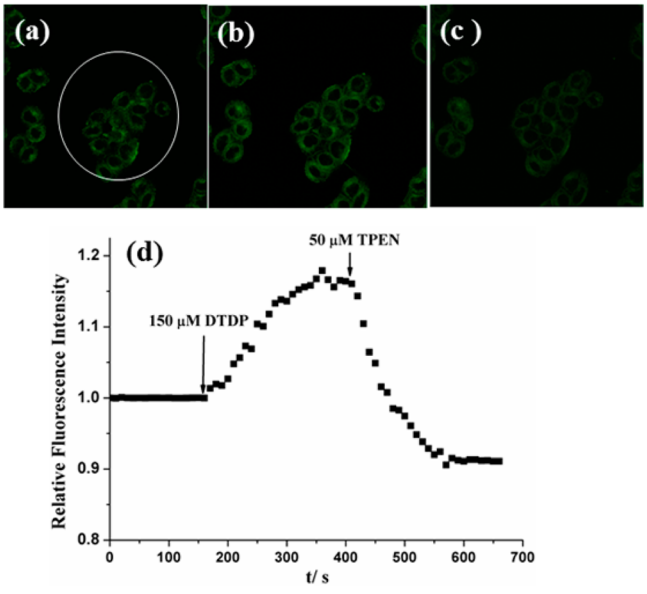

Figure 6. (a–c) 2PM images of 0.5 μM QZn-labeled HeLa cells (a) before and (b) after addition of 150 μM DTDP to the imaging solution and (c) after addition of 50 μM TPEN to (b). (d) Relative 2PEF intensity of QZn-loaded HeLa cells as a function of time. The 2PEF intensities were collected at 500–570 nm upon excitation at 820 nm with femtosecond pulses.

solubility, pH insensitivity, and low cytotoxicity. This probe exhibited a moderate 2P action cross section value of 51 GM at 820 nm. The probe was successfully applied for sensitively monitoring the fluctuation of intracellular free zinc ions in real time under 2PM. We anticipate quinoline to be a good 2P scaffold to develop various 2P probes and QZn could be a potential tool to study the roles of zinc ions in physiology and pathology by two-photon microscopy.

■ ASSOCIATED CONTENT

Supporting Information

Water solubility test, spectroscopic measurements, TD-DFT calculation results, determination of apparent dissociation constants. Two-photon action cross section spectra of QZn and QZn-Zn^{2+} complex, photostability of QZn under two-photon microscopy, and spatial localization of QZn in HeLa cells. This material is available free of charge via the Internet at http://pubs.acs.org.

■ AUTHOR INFORMATION

Corresponding Author

*E-mail: zhhliu@whu.edu.cn. Phone: 86-27-8721-7886. Fax: 86-27-6875-4067.

Notes

The authors declare no competing financial interest.

■ ACKNOWLEDGMENTS

This work was supported by the National Natural Science Foundation of China (No. 21375098), the National Basic Research of China (973 program, No. 2011CB910403), and the Program for New Century Excellent Talents in University (NCET-11-0402).

■ REFERENCES

(1) Frederickson, C. J.; Koh, J. Y.; Bush, A. I. *Nat. Rev. Neurosci.* **2005**, *6*, 449–462.

(2) Vallee, B. L.; Falchuk, K. H. *Physiol. Rev.* **1993**, *73*, 79−118.
(3) Hambidge, M. *J. Nutr.* **2000**, *130*, 1344S−1349S.
(4) Vallee, B. L.; Auld, D. S. *Acc. Chem. Res.* **1993**, *26*, 543−551.
(5) Nakashima, A. S.; Dyck, R. H. *Brain Res. Rev.* **2009**, *59*, 347−373.
(6) Parasad, S. A. *Annu. Rev. Nutr.* **1985**, *5*, 341−365.
(7) Ghosh, S. K.; Kim, P.; Zhang, X. A.; Yun, S. H.; Moore, A.; Lippard, S. J.; Medarova, Z. *Cancer Res.* **2010**, *70*, 6119−6127.
(8) Cummings, J. E.; Kovacic, J. P. *J. Vet. Emerg. Crit. Care* **2009**, *19*, 215−240.
(9) Koike, T.; Watanabe, T.; Aoki, S.; Kimura, E.; Shiro, M. *J. Am. Chem. Soc.* **1996**, *118*, 12696−12703.
(10) Sensi, S. L.; Ton-That, D.; Weiss, J. H.; Rothe, A.; Gee, K. R. *Cell Calcium* **2003**, *34*, 281−284.
(11) Hirano, T.; Kikuchi, K.; Urano, Y.; Nagano, T. *J. Am. Chem. Soc.* **2002**, *124*, 6555−6562.
(12) Buccella, D.; Horowitz, J. A.; Lippard, S. J. *J. Am. Chem. Soc.* **2011**, *133*, 4410−4114.
(13) Lin, W.; Buccella, D.; Lippard, S. J. *J. Am. Chem. Soc.* **2013**, *135*, 13512−13520.
(14) Wang, J.; Xiao, X.; Zhang, Z.; Qian, X.; Yang, Y.; Xu, Q. *J. Mater. Chem.* **2005**, *15*, 2836−2839.
(15) Xue, L.; Li, G.; Zhu, D.; Liu, Q.; Jiang, H. *Inorg. Chem.* **2012**, *51*, 10842−10849.
(16) Helmchen, F.; Denk, W. *Nat. Methods* **2005**, *2*, 932−940.
(17) Zipfel, W. R.; Williams, R. M.; Webb, W. W. *Nat. Biotechnol.* **2003**, *21*, 1369−1377.
(18) Taki, M.; Wolford, J. L.; O'Halloran, T. V. *J. Am. Chem. Soc.* **2004**, *126*, 712−713.
(19) Huang, C.; Qu, J.; Qi, J.; Yan, M.; Xu, G. *Org. Lett.* **2011**, *13*, 1462−1465.
(20) Kim, H. M.; Seo, M. S.; An, M. J.; Hong, J. H.; Tian, Y. S.; Choi, J. H.; Kwon, O.; Lee, K. J.; Cho, B. R. *Angew. Chem.* **2008**, *120*, 5245−5248.
(21) Masanta, G.; Lim, C. S.; Kim, H. J.; Han, J. H.; Kim, H. M.; Cho, B. R. *J. Am. Chem. Soc.* **2011**, *133*, 5698−5700.
(22) Baek, N. Y.; Heo, C. H.; Lim, C. S.; Masanta, G.; Cho, B. R.; Kim, H. M. *Chem. Commun.* **2012**, *48*, 4546−4548.
(23) Dong, X.; Heo, C. H.; Chen, S.; Kim, H. M.; Liu, Z. *Anal. Chem.* **2014**, *86*, 308−311.
(24) Frisch, M. J.; Trucks, G. W.; Schlegel, H. B.; Scuseria, G. E.; Robb, M. A.; Cheeseman, J. R.; Scalmani, G.; Barone, V.; Mennucci, B.; Petersson, G. A.; Nakatsuji, H.; Caricato, M.; Li, X.; Hratchian, H. P.; Izmaylov, A. F.; Bloino, J.; Zheng, G.; Sonnenberg, J. L.; Hada, M.; Ehara, M.; Toyota, K.; Fukuda, R.; Hasegawa, J.; Ishida, M.; Nakajima, T.; Honda, Y.; Kitao, O.; Nakai, H.; Vreven, T.; Montgomery, J. A., Jr..; Peralta, J. E.; Ogliaro, F.; Bearpark, M.; Heyd, J. J.; Brothers, E.; Kudin, K. N.; Staroverov, V. N.; Kobayashi, R.; Normand, J.; Raghavachari, K.; Rendell, A.; Burant, J. C.; Iyengar, S. S.; Tomasi, J.; Cossi, M.; Rega, N.; Millam, N. J.; Klene, M.; Knox, J. E.; Cross, J. B.; Bakken, V.; Adamo, C.; Jaramillo, J.; Gomperts, R.; Stratmann, R. E.; Yazyev, O.; Austin, A. J.; Cammi, R.; Pomelli, C.; Ochterski, J. W.; Martin, R. L.; Morokuma, K.; Zakrzewski, V. G.; Voth, G. A.; Salvador, P.; Dannenberg, J. J.; Dapprich, S.; Daniels, A. D.; Farkas, Ö.; Foresman, J. B.; Ortiz, J. V.; Cioslowski, J.; Fox, D. J. *Gaussian 09*, Revision A.02 ed.; Gaussian, Inc.: Wallingford CT, 2009.
(25) Dong, X.; Yang, Y.; Sun, J.; Liu, Z.; Liu, B. F. *Chem. Commun.* **2009**, *26*, 3883−3885.
(26) Dong, X.; Han, J. H.; Heo, C. H.; Kim, H. M.; Liu, Z.; Cho, B. R. *Anal. Chem.* **2012**, *84*, 8110−8113.
(27) Lee, S. K.; Yang, W. J.; Choi, J. J.; Kim, C. H.; Jeon, S. J.; Cho, B. R. *Org. Lett.* **2005**, *7*, 323−326.
(28) Xu, C.; Webb, W. W. *J. Opt. Soc. Am. B* **1996**, *13*, 481−491.
(29) Demas, J. N.; Crosby, G. A. *J. Phys. Chem.* **1971**, *75*, 991−1024.
(30) Chung, C.; Srikun, D.; Lim, C. S.; Chang, C. J.; Cho, B. R. *Chem. Commun.* **2011**, *47*, 9618−9820.
(31) Lim, C. S.; Das, S. K.; Yang, S. Y.; Kim, E. S.; Chun, H. J.; Cho, B. R. *Anal. Chem.* **2013**, *85*, 9288−9295.
(32) Adronov, A.; Fréchet, J. M. J.; He, G. S.; Kim, K.-S.; Chung, S.-J.; Swiatkiewicz, J.; Prasad, P. N. *Chem. Mater.* **2000**, *12*, 2838−2841.
(33) Yu, H.; Xiao, Y.; Jin, L. *J. Am. Chem. Soc.* **2012**, *134*, 17486−17489.
(34) Mao, G. J.; Wei, T. T.; Wang, X. X.; Huan, S. Y.; Lu, D. Q.; Zhang, J.; Zhang, X. B.; Tan, W.; Shen, G. L.; Yu, R. Q. *Anal. Chem.* **2013**, *85*, 7875−7881.
(35) Brousmiche, D. W.; Serin, J. M.; Fréchet, J. M. J.; He, G. S.; Lin, T.-C.; Chung, S. J.; Prasad, P. N. *J. Am. Chem. Soc.* **2003**, *125*, 1448−1449.
(36) Andrade, C. D.; Yanez, C. O.; Rodriguez, L.; Belfield, K. D. *J. Org. Chem.* **2010**, *75*, 3975−3982.
(37) Yao, S.; Schafer-Hales, K. J.; Belfield, K. D. *Org. Lett.* **2007**, *9*, 5645−5648.
(38) Kim, H. M.; Cho, B. R. *Acc. Chem. Res.* **2009**, *42*, 863−872.
(39) Kiyose, K.; Kojima, H.; Urano, Y.; Nagano, T. *J. Am. Chem. Soc.* **2006**, *128*, 6548−6549.
(40) Komatsu, K.; Kikuchi, K.; Kojima, H.; Urano, Y.; Nagano, T. *J. Am. Chem. Soc.* **2005**, *127*, 10197−10204.
(41) Komatsu, K.; Urano, Y.; Kojima, H.; Nagano, T. *J. Am. Chem. Soc.* **2007**, *129*, 13447−13454.
(42) Zhang, X.; Chi, L.; Ji, S.; Wu, Y.; Song, P.; Han, K.; Guo, H.; James, T. D.; Zhao, J. *J. Am. Chem. Soc.* **2009**, *131*, 17452−17463.
(43) Liu, Y.; Dong, X.; Sun, J.; Zhong, C.; Li, B.; You, X.; Liu, B.; Liu, Z. *Analyst* **2012**, *137*, 1837−1845.
(44) Tanaka, K.; Miura, T.; Umezawa, N.; Urano, Y.; Kikuchi, K.; Higuchi, T.; Nagano, T. *J. Am. Chem. Soc.* **2001**, *123*, 2530−2536.
(45) Zhang, H.; Fan, J.; Wang, J.; Zhang, S.; Dou, B.; Peng, X. *J. Am. Chem. Soc.* **2013**, *135*, 11663−11669.
(46) Zhang, H.; Fan, J.; Wang, J.; Dou, B.; Zhou, F.; Cao, J.; Qu, J.; Cao, Z.; Zhao, W.; Peng, X. *J. Am. Chem. Soc.* **2013**, *135*, 17469−17475.
(47) Su, H.; Chen, X.; Fang, W. *Anal. Chem.* **2014**, *86*, 891−899.
(48) He, H.; Mortellaro, M. A.; Leiner, M. J. P.; Young, S. T.; Fraatz, R. J.; Tusa, J. K. *Anal. Chem.* **2003**, *75*, 549−555.
(49) Qian, W. J.; Aspinwall, C. A.; Battiste, M. A.; Kennedy, R. T. *Anal. Chem.* **2000**, *72*, 711−717.
(50) Meeusen, J. W.; Tomasiewicz, H.; Nowakowski, A.; Petering, D. H. *Inorg. Chem.* **2011**, *50*, 7563−7573.
(51) Nguyen, D. M.; Wang, X.; Ahn, H. Y.; Rodriguez, L.; Bondar, M. V.; Belfield, K. D. *ACS Appl. Mater. Interfaces* **2010**, *2*, 2978−2981.
(52) Meeusen, J. W.; Nowakowski, A.; Petering, D. H. *Inorg. Chem.* **2012**, *51*, 3625−3632.
(53) Barnett, B. L.; Kretschmar, H. C.; Hartman, F. A. *Inorg. Chem.* **1977**, *16*, 1834−1838.
(54) Aizenman, E.; Stout, A. K.; Hartnett, K. A.; Dineley, K. E.; McLaughlin, B.; Reynolds, I. J. *J. Neurochem.* **2000**, *75*, 1878−1788.